Available online at www.sciencedirect.com
SCIENCE DIRECT®
Sensors and Actuators B 106 (2005) 563–571
SENSORS AND ACTUATORS B CHEMICAL
www.elsevier.com/locate/snb

Experimental and theoretical studies of indium oxide gas sensors fabricated by spray pyrolysis

V. Golovanov[a], Matti A. Mäki-Jaskari[b,*], Tapio T. Rantala[b], G. Korotcenkov[c], V. Brinzari[c], A. Cornet[d], J. Morante[d]

[a] *South-Ukrainian University, Staroportofrankovskaya Str. 26, 65008 Odessa, Ukraine*
[b] *Tampere University of Technology, P.O. Box 692, FIN-33101, Tampere, Finland*
[c] *Technical University, Bld. Stefan cel Mare, 168, 2004 Chisinau, Moldova*
[d] *Department of Electronics, University of Barcelona, Marti i Franqus 1, 08028 Barcelona, Spain*

Received 8 April 2004; received in revised form 2 July 2004; accepted 28 July 2004
Available online 22 September 2004

Abstract

Surface structures of In_2O_3 films have been studied by employing experimental methods for surface characterization together with theoretical modeling for geometries, electronic structures and surface energetics. Polycrystalline In_2O_3 films deposited by spray pyrolysis were analyzed by using XRD, HRTEM and XPS methods. It is found that the most abundant (4 0 0) surface face reconstructs considerably leading to formation of surface mono-oxygen and di-oxygen forms. This uppermost surface layer exhibit high ability to reduction/oxidation processes during the thermal treatment. The unsaturated indium ions appearing at the reconstructed surface serve as the active sites for the chemisorbed oxygen species. Therefore, the mechanisms of In_2O_3 sensitivity to reducing gases include both "redox" and catalytic effects in a very thin surface layer. On the other hand, response of In_2O_3-based gas sensors to oxidizing gases is limited by diffusion type processes.

Keywords: Surface properties; Gas sensing; In_2O_3.

1. Introduction

Among various metal oxides In_2O_3 appears to be rather attractive in a view of excellent sensitivity and selectivity to combustion gases and typical air pollutants (CO, CH_4, H_2, NO_x) [1–4]. Indium oxide have demonstrated a performance better than SnO_2 in detection of ozone [5–9] and offers a new advantage in designing of metal oxide-based gas sensors linked with essential difference in electrophysical and chemical properties between SnO_2 and In_2O_3 [10–12].

Indium oxide material has recently been a subjected of a number of experimental studies [13–21]. The sensing mechanism of In_2O_3 is attributed mainly to oxidation/reduction (redox) mechanism [22–24]. This postulation is based on the assumption that chemisorbed oxygen species do not exist at the surface of In_2O_3 because of its transformation into lattice atomic oxygen immediately after adsorption. However, correlation between surface structure and gas response properties established for In_2O_3 films [25,26] suggests that the mechanism of In_2O_3 sensitivity is more complicated and cannot be limited to redox mechanism, only. Because of the these challenges it is important to attempt to consider In_2O_3 surfaces also using theoretical methods once experimentally confirmed model for sensor surface is constructed.

In the present paper polycrystalline In_2O_3 films have been studied employing experimental methods of surface characterization along with theoretical modeling of the In_2O_3 surface. For deposition of In_2O_3 we chose spray pyrolysis technique which offers possibilities for structural control [27–29]. Theoretical modeling was done em-

* Corresponding author. Tel.: +358 3 365 4226; fax: +358 3 365 2600.
E-mail addresses: alban@te.net.ua (V. Golovanov), matti.maki-jasakari@tut.fi (M.A. Mäki-Jaskari).

0925-4005/$ – see front matter © 2004 Elsevier B.V. All rights reserved.
doi:10.1016/j.snb.2004.07.026

ploying density functional method. As an effective surface model, an oxygen deficient (4 0 0) surface with a presence of strongly bound mono-oxygen and di-oxygen species is considered.

2. Experimental details

In_2O_3 films with thickness 10–400 nm were deposited from InCls-water solution. Precursor concentration in sprayed solution was varied from 0.05 to l.0 M. In_2O_3 films were deposited onto silicon (1 1 1) and alumina ceramic substrates heated at 300–550 °C. The films were provided with Au-contacts. The distance between the electrodes was equaled to ∼2–3 mm.

The surface morphology and chemical composition were examined using X-ray diffraction (XRD) (6/26 mode), Atomic Force Microscopy (AFM), High Resolution Transmission Electron Microscopy (HRTEM), X-ray Photoelectron Spectroscopy (XPS) and Raman Spectroscopy methods. For these purposes, we used such instruments as diffractometer Siemens D5000 (CuKa); Philips CM30 SuperTwin transmission electron microscope operating at 300 keV; scanning electron microscopes Jeol JSM840 and Philips XL30; MultiMode Scanning Probe Microscope with Nanoscope Hla Controller of Digital Instruments; X-ray Photoelectron hemispherical electrostatic analyzer Omicron EA 125; and Jobin E6400 Micro-Raman instrument, equipped with a He-Ne laser (632.8 nm) and an argon ion laser (514.5 nm).

Degree of film texturing were calculated as a ratio I(4 0 0)/I(2 2 2) of the most intensive peaks in XRD patterns. Grain size was calculated, on the basis of XRD data, using standard Sherrer's formula.

Gas response to CO, H_2 (0.1–0.5%) and ozone (<l ppm) were measured in steady-state and transient modes both in wet (35–50% RH) and dry atmospheres (1–2% RH). The operating temperature of the sensors was adjusted between 25 and 450 °C during the measurements. The gas response was calculated as a resistance ratio R(ozone)/R(air) for the ozone detection, and R(air)/R(CO,H_2) for the CO or H_2 detection. The volume of the measurement cell was smaller than 0.5 cm^{-3}. In this case, exchange time of gas atmosphere was smaller than 2–4 s. Response and recovery times were estimated on the 0.9 level and 0.1 level from the steady-state film resistance, respectively.

The fitting procedure of O1s peak was applied assuming three peaks composed of Voigt curves with Lorentzian contribution of less than 10% in total FWHM and constant (independent of sample) energy difference between them. The In 4d peak was assumed to consist of two doublets. Parameters of the In 4d peak fit were taken from [30]. A Shireley background substraction was included in fitting procedure. For calculation of the O/In ratio, we used the integrated total area of oxygen and indium peaks normalized according to their photoionization cross-sections.

3. Structural and gas response characterization of the In_2O_3 films

Detailed structural analysis indicates that the In_2O_3 films deposited by spray pyrolysis belong to cubic *Ia3* space group with a = 1.0118 nm. Grain size in these films depends on both T_{pyr} and film thickness. For example, increase of film thickness from 20–30 to 400 nm results in grain size increase from 8–15 to 60–80 nm.

Comparison of the experimentally observed XRD patterns with corresponding patterns of In_2O_3 powders [31] confirm that In_2O_3 films, deposited at T_{pyr} < 350 °C, are randomly oriented. The films deposited at T_{pyr} > 350 °C, have a pronounced columnar structure with a characteristic grain size of ∼30–40 nm in the vertical direction. A typical HRTEM image of the deposited films is shown in Fig. 1. Results of the HRTEM analysis, demonstrate that such films are compactly packed and highly textured with predominant crystallite orientation in the [0 0 1] direction, perpendicular to the substrate. The terminal faces of the crystallites correspond to (4 0 0) atomic plane and the lateral plane correspond to (1 0 0) surface, which has essentially the same structure. A typical XRD pattern for In_2O_3 films deposited at T_{pyr} > 400 °C is shown in Fig. 2. It is seen that the films with thickness ∼200 nm exhibit intensity of the (4 0 0) reflection about 20–30 times higher than that of the second strongest (2 2 2) reflection. For comparison, ratio I(4 0 0)/I(2 2 2) for randomly oriented In_2O_3 powders is equaled 0.25. The degree of texturing increases with increasing film thickness, and exceeds 90%.

Some results concerning In_2O_3 gas response to reducing and oxidizing gases are presented in references [9,32,33]. These results have shown that detection of indicated gases takes place through different mechanisms. The sharp distinction of the sensing mechanisms to oxidizing and reducing gases is reflected in different temperatures, at which maximum of sensitivity has been observed (e.g. T ∼ 150–300 °C and T > 400–450 °C for oxidizing and reducing gases, respectively).

The study of gas sensing behavior of In_2O_3 films with different thickness and grain sizes suggests that a sensing response to oxidizing gases is limited by both chemisorption and diffusion processes. There is a typical regularity associated: the smaller grain size the higher sensor sensitivity. In more detail, the dependence of response time on grain size corresponds to quadratic law, indicating that diffusion type processes can be rate-determining [32]. Increase of the film thickness from 20 to 400 nm leads to decrease of gas response to ozone with a factor larger than 100 (see Fig. 3). It is noticeable, that during ozone detection in dry air a relation $t_{rec} \gg t_{res}$ was observed (see Fig. 4), which is typical for mechanisms controlled by chemisorption/diffusion type processes. In wet atmosphere the influence of film structure on time constants of gas response to ozone is sharply decreased. In this case, the response and recovery times became comparable ($\tau_{res} \sim \tau_{rec}$) which indicates to surface character of the

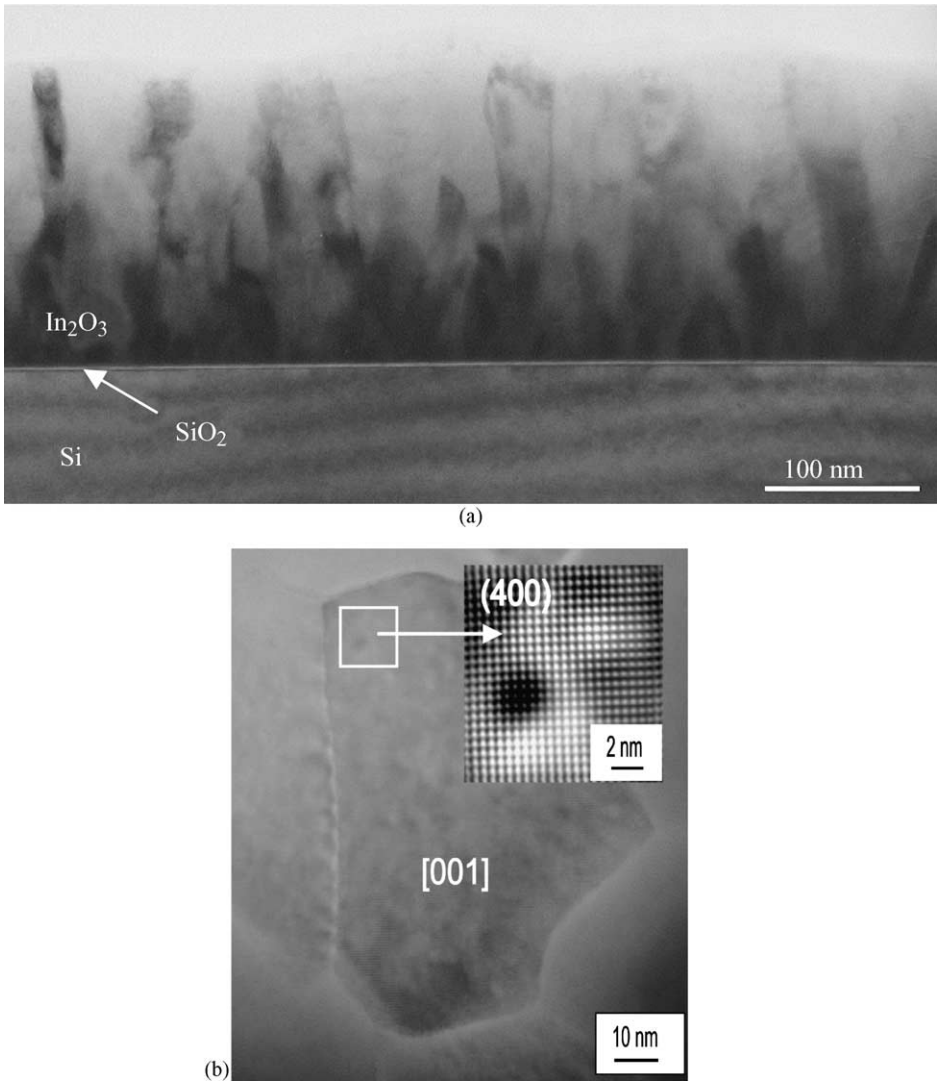

Fig. 1. HRTEM micrograph of the In_2O_3 film ($d \sim 200$ nm): (a) cross-section displaying its columnar structure and (b) planar view with a diffractogram demonstrating its preferred (1 0 0) orientation.

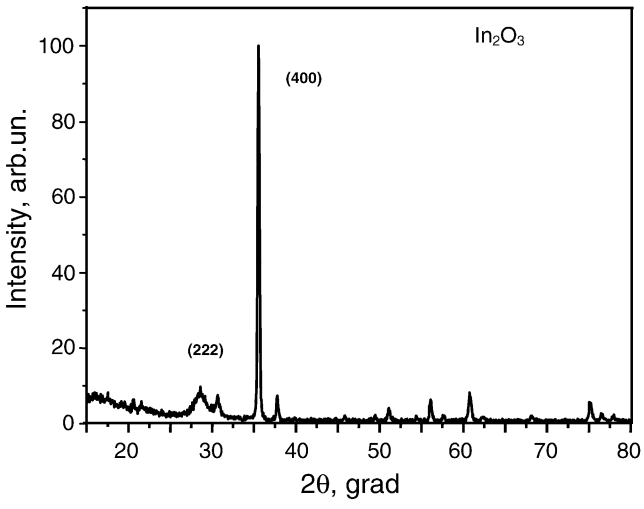

Fig. 2. Typical XRD patterns of In_2O_3 films deposited at $T_{pyr} > 400\,^{\circ}C$.

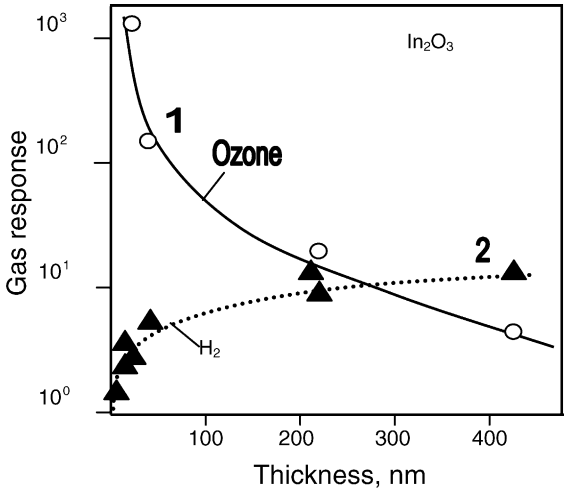

Fig. 3. Dependencies of gas response to (1) ozone ($T_{oper} = 270\,^{\circ}C$) and (2) H_2 ($T_{oper} = 370\,^{\circ}C$) on In_2O_3 film thickness.

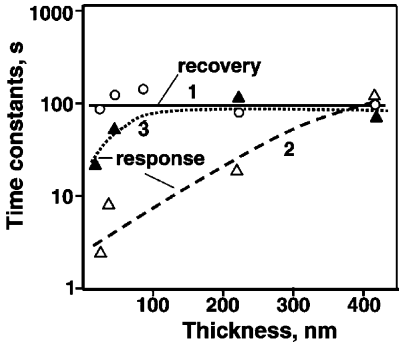

Fig. 4. Recovery (1) and response (2,3) times for ozone detection vs. thickness of the In_2O_3 films (T_{pyr} =475 °C, T_{oper} = 270 °C); (1,2) dry air, (3) wet air.

reactions, as well as on the significant role of water in this process.

Contribution of film structures in detection of the reducing gases is weaker. The decrease of thickness, grain size, and degree of texturing has no essential influence on the gas response of the In_2O_3 films, during the detection of the reducing gases (see Fig. 3). Moreover, the sensitivity of In_2O_3-based gas sensors to the reducing gases has a noticeable value even for crystallite size exceeding 80–100 nm. The sheet resistance of In_2O_3 films in an atmosphere of reducing gases practically does not depend on the crystallite size, while exposure to oxidizing gases demonstrates significant role of the intergranular barriers in the conductance behavior. From this it is clear that crystallite size does not determine the gas response of In_2O_3-based gas sensors to reducing gases. At that, during the detection of reducing gases we observe correlation $\tau_{rec} \sim \tau_{res}$, typical for mechanisms controlled by reactions of surface catalysis and surface reduction [33]. The reversible change of the Raman spectra in measurement cycle air—>{CO + air)—>air (see Fig. 5) demonstrates that reconstruction of the In_2O_3 nanoscaled grain structure takes place in reducing atmosphere at $T > 200$ °C already. The essential changes of the Raman spectra in the range of bulk modes indicate that observed structure modification occurs throughout the grain, and therefore, cannot be associated with adsorption only. At low temperatures ($T < 200$ °C), where the probability of CO adsorption is high, changes in the in spectra have not been observed. These facts indicate that observed changes in the Raman spectra are caused by the interaction of CO with the lattice oxygen, i.e. by "reduction" of In_2O_3 lattice. It is not reasonable to associate the observed transformation in the Raman spectra with the chemisorbed oxygen, since the change of the temperature Toper, (which obviously alters the concentration of the chemisorbed oxygen) had no effect on the measured Raman spectra. Based on the analysis of gas response properties, it was concluded that sensing mechanisms of the deposited In_2O_3 films to reducing gases include processes occurring in a thin surface layer. The XPS spectroscopy was applied in order to estimate the characteristics of this layer in more detail.

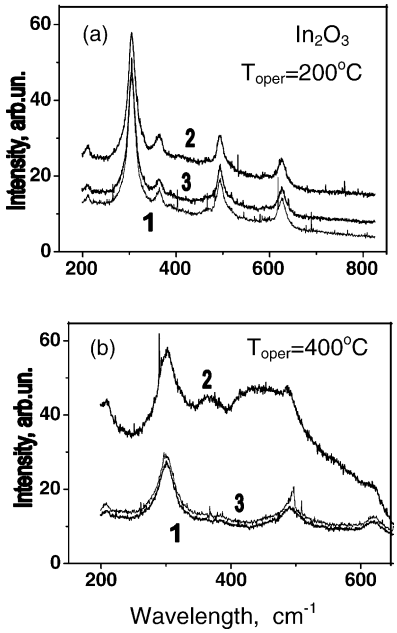

Fig. 5. Influence of the surrounding atmosphere on Raman spectra of In_2O_3 films deposited by spray pyrolysis: (a) T_{oper} = 200 °C; (b) T_{oper} = 400 °C. (1) air before treatment; (2) treatment in (10%CO + N_2) atmosphere; (3) air after treatment.

The XPS spectra of O1s core level electrons, measured from In_2O_3 thin film deposited by spray pyrolysis, displayed three peaks with binding energies of 530.5, 532.1 and 533.5 eV (shown in Fig. 6a). The first (main) peak, with maximum at 530.5 eV, corresponds to the bulk lattice oxygen. The nature of the third peak with maximum at 533.5 eV complies with chemisorbed oxygen and water related species. Behavior of the second peak (at 532.1 eV) under different surface treatments, were associated to oxygen that forms a rather stable phase in the terminal and subsurface area of the In_2O_3 films. The analysis of XPS spectra (shown in Fig. 6b), indicated that terminal layers of In_2O_3 films redialy reduces and exhibit deficiency of lattice oxygen, which corresponds to formula In_xO_y, with $x, y = 1$. It is noticeable, that such non-stoichiometric state of the surface remains stable even after heat treatment in oxygen atmosphere. Annealing at elevated temperature ($T > 1000$ °C) restores the stoichiometry corresponding to the ideal In_2O_3 structure. Our last experiments, conducted using synchrotron radiation photoelectron spectroscopy (SRPS), allowed us to analyze changes occurring at the films uppermost layer during adsorption/desorption processes. These measurements have supported conclusion about the formation of lattice oxygen deficient (4 0 0) surface although indicates a rather large amount of oxygen (O/In $\sim$ 1) within a depth of a few Angstroms. A separate article will be devoted to a discussion of these results. In spite of the absence of high accuracy in the determination of the O/In ratio, the main result is obvious – a sharp decrease of stoichiometric oxygen atom concentration in the surface vicinity.

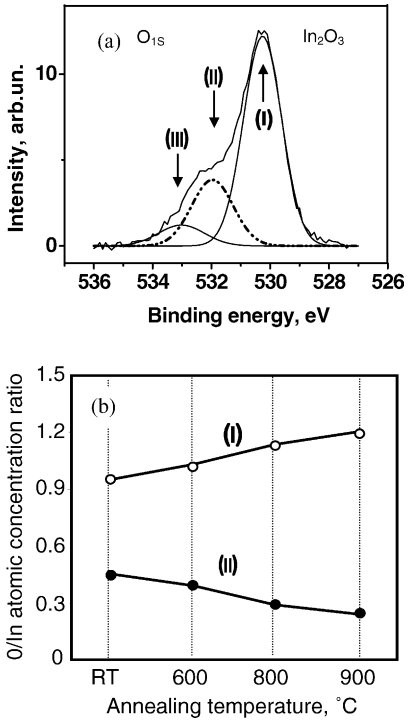

Fig. 6. O1s core level XPS spectrum of In_2O_3 thin film, displaying three peaks with binding energies of 530.5 eV (I), 532.1 eV (II) and 533.5 eV (III) (a) and normalized O/In ratio for the first (main) and second deconvoluted O_{1s} core level peaks (b) in dependence on annealing temperature.

4. Theoretical modeling of In_2O_3 surface

The experimental results demonstrate that sensing mechanisms in In_2O_3 films include chemisorption, catalytic and redox effects. Redox effects imply participation of the lattice oxygen in the sensing mechanism with changes in stoichiometry, which can be accompanied by surface reconstruction occurring already at low temperatures. This conclusion correlates with the non-stoichiometry as detected by XPS of surface layers of the In_2O_3 sensor films. Especially in detection of ozone, film and grain surfaces are expected to be able to influence substantially. As discussed above, the (4 0 0) surface represents the structure of the most common face of In_2O_3 crystallites. Together with the predicted surface composition, these results offer an important starting point to model computationally effective surface geometry and its influence on electronic and energetic properties.

Our theoretical modeling is based on ab initio-density functional calculations with plane wave basis and pseudopotentials (CASTEP/CETEP code) [34]. Each indium atom contains 13 and each oxygen atom 6 valence electrons. By using ultrasoft pseudopotentials [35] the plane wave basis set could be limited to cut-off 400 eV. To sample the Brillouin zone, six symmetrized Monkhorst-Pack *k*-points [36] were used for a primitive unit cell ($In_{16}O_{24}$). The electronic interactions were taken into account within the generalized-gradient approximation [37]. The possibility of spin-polarization was tested in separate calculations. Optimization of bulk In_2O_3 lattice was performed, yielding cell parameters (a = 1.03 nm) in close agreement with experimental lattice constant. Indium oxide surfaces were modeled by using a three dimensionally periodic slab model (shown in Figs. 7 and 8) with a vacuum of 10 Å between the surfaces. The slabs, containing three indium layers, were cut from the optimized In_2O_3 lattice and as a consequence they have less symmetry. Associated symmetry (P 21/c 2/c 2/a) were utilized to restrict geometry and to speed up electronic structure calculations. The centermost indium atoms were not allowed to relax from bulk positions. The total number of atoms of the different surface slab models varies from 48 to 72, which quite dramatically increases the computational cost. In separate test calculations, without any symmetry restrictions and with increased slab thickness, it was noticed that these approximations do not change energetics and surface relaxation significantly. This result can be attributed to the relatively high stability of the ionic systems considered.

Fig. 7 shows a model of ideal (4 0 0) face of In_2O_3, with all surface bridging oxygens, classified to three types. The terminal layer distances from the indium atomic plane are 1.4 Å (OI form), 1.3 Å (OII form) and 0.95 Å (OIII form). Calculations indicate that this type of surface is not stable, but stabilizes by releasing its OII oxygens. Surface reconstruction leads to the bonding between neighboring OII oxygens, resulting in formation of surface molecular oxygen, which almost completely desorbs from the surface. Similar formation of weakly bound molecular oxygen species were observed by starting from other geometries with the same amount of oxygen at the surface. This result implies that certain external conditions, like high oxygen pressure with an injection of additional electrons at surface, may be required for stabilization of the full oxygen coverage.

To consider possible stable (4 0 0) surface geometries, we start with highly reduced surfaces with only one type of oxygen. The oxygen coverage is then 0.04 $Å^{-2}$ (In_xO_y; x = 2, y = 1). At such surfaces, each surface indium cation has a single bond to surface bridging oxygen, and each surface oxygen atom is bound to two surface indium cations. Because of the freedom in surface geometry and supply of charge from cations, the surface oxygens are expected to have strong bonds and large adsorption energies. The most favorable oxygen adsorbates were found to be type OIII oxygens. They have an adsorption energy exceeding 1.4 eV, with respect to free spin-polarized oxygen molecule. For OII and OI types of surface oxygens, corresponding energies are only slightly smaller; 1.35 and 1.3 eV, respectively. Other attachments of individual bridging oxygens to indium atoms lead to less stable systems (and will not be considered here for the sake of brevity). The adsorbed OIII is associated with In–O–In bond angle (117°), which is characteristic to sp^2 hybridization.

When there is larger amount of surface oxygen, like in the experimentally predicted cases (coverage 0.08 $Å^{-2}$), different types of oxygens are present at the surface. Below the coverage of 0.08 $Å^{-2}$, stable surface geometries which are essentially combinations of the different types of surface

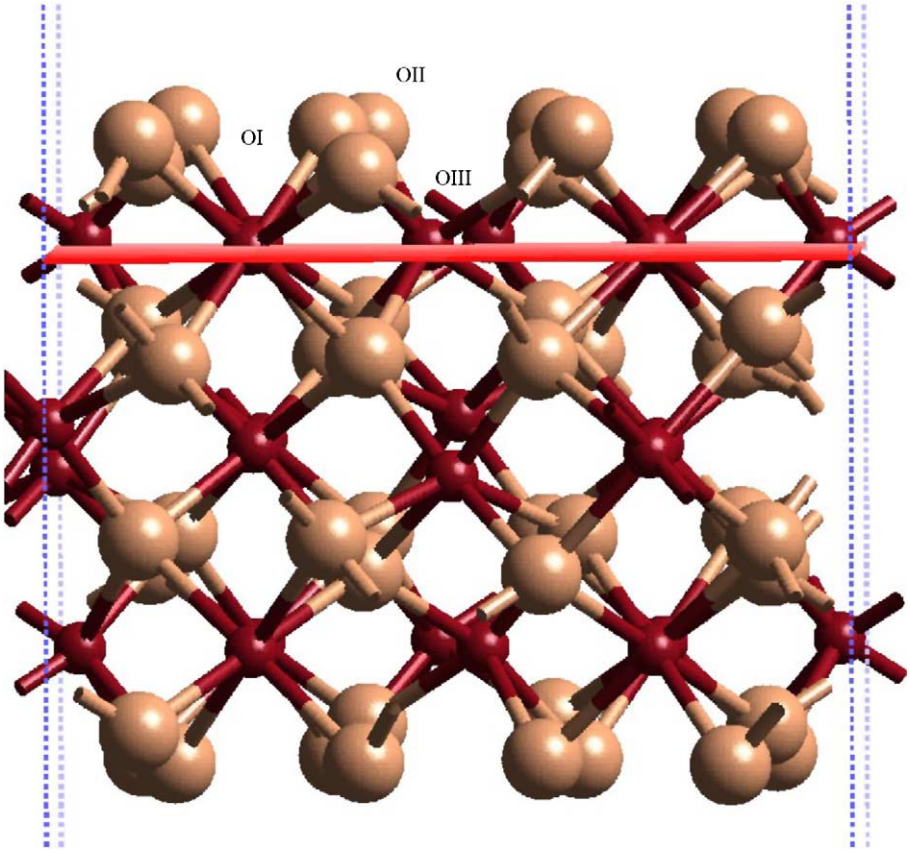

Fig. 7. The model of the In_2O_3 unit cell demonstrating ideal (4 0 0) face with three different types of bridging oxygen distanced from the indium atomic plane on 1.43 Å (O(I) form), 1.31 Å (O(II) form) and 0.95 Å (O(III) form). The smaller spheres represent indium atoms and the larger ones oxygen atoms.

oxygen geometries were found. These surface geometries do not have noticeable changes in the optimized surface geometry and adsorption energies with respect to the above classification. When surface oxygen coverage is increased so that some of the two types of oxygens are present at surface (coverage 0.08 $Å^{-2}$), a combination of OIII + OII is found to be more stable than other combinations OIII + OI and OII + OI. The adsorption energy of OII, at the surface with OIII, is 1.2 eV/atom. With respect to the oxide surface without any surface oxygen, the resulting OII + OIII surface has adsorption energy of 1.3 eV/atom. These adsorption energies are close to the adsorption energies of the individual bridging oxygens (1.3–1.4 eV).

A comparison of formation of the different surfaces can be made in terms of surface energies. Surface energies are estimated by subtracting from the energy of the surface slab corresponding total energy of bulk In_2O_3, from which corresponding energy of oxygens absent were subtracted. The contribution of oxygens are estimated taking into account the extreme limits of chemical potentials of indium (μ_{In}) and oxygen (μ_O) atoms [38]. The surface energy (E_{surf}) is evaluated from

$$E_{surf} = \frac{(E_{sl} - (N_{In}\mu_{In_2O_3}/2) - (N_O - (3N_{In}/2))\mu_O)}{2A}, \quad (1)$$

where E_{sl} is the total energy of a slab with a surface area A, containing N_{In} indium and N_O oxygen atoms. The chemical potential of bulk indium oxide is denoted by $\mu_{In_2O_3}$, which is obtained from the evaluated total energy. As a first limit, μ_O may be estimated as a half of the total energy of free oxygen molecule. This limit is attributed to oxygen rich surface, since it can be assumed that oxygen rich surfaces in equilibrium are closer to this limit than oxygen deficient surfaces. An opposite limit for μ_O were evaluated from $\mu_O = (\mu_{In_2O_3} - 2\mu_{In})/3$, where μ_{In} is obtained from calculated total energy of indium metal crystal (symmetry I 4/m 2/m 2/m). This limit corresponds to oxygen deficient case, where indium bulk phase can coexist. Evaluated surface energies, corresponding to a limit in which bulk In_2O_3 phase is in equilibrium with oxygen gas environment, were 2.3 J/m^2 in the case of OIII surface and 1.6 J/m^2 in the case of the OII + OIII surface. In the other limiting case in which bulk In_2O_3 is in equilibrium with indium metal phase, the limits were 1.5 J/m^2 in the case of OIII surface and 2.4 J/m^2 in the case of OII + OIII. Surface energies of the surfaces are listed in Table 1, which indicates that OII + OIII, OIII or their combination are indeed most stable surfaces.

The calculated results are in agreement with the analysis of deposited indium oxide films, which point out formation of energetically stable lattice oxygen-deficient (4 0 0) surface.

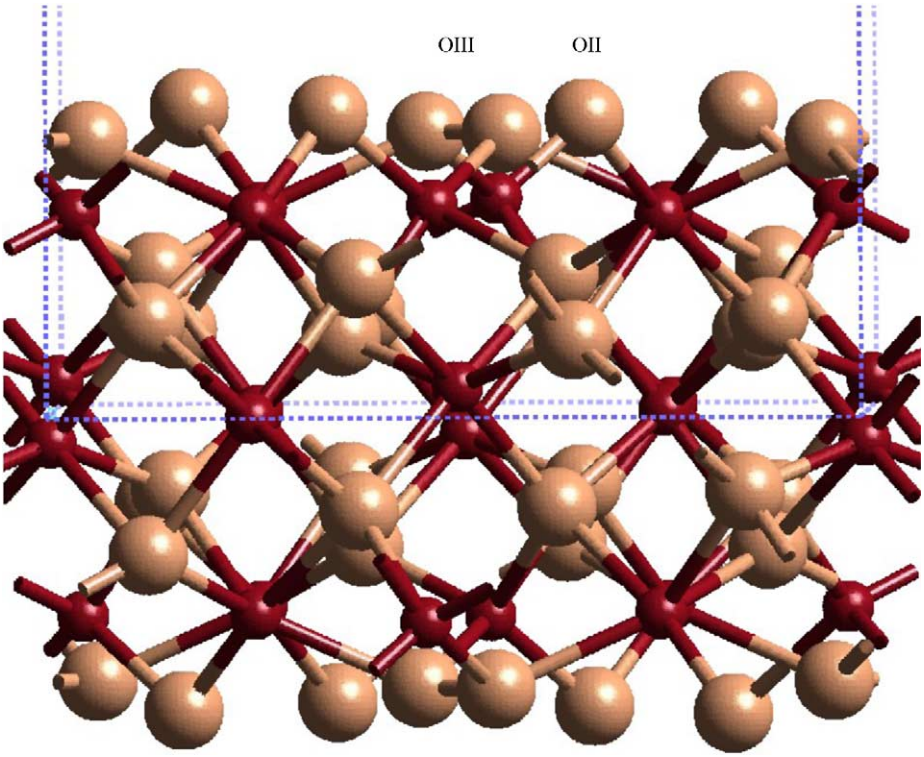

Fig. 8. Reconstruction of the In_2O_3 (4 0 0) atomic face leading to formation of surface oxygen molecules at non-stoichiometric OII + OIII surface. The symbols are same as in Fig.7.

Based on the calculations, a surface with OII + OIII oxygens is a representative model for In_2O_3 surface. At this surface, which shown in Fig. 8, the surface oxygens are reconstructed considerably forming surface oxygen molecules (peroxide). It is noticeable that that the adsorbed oxygens are not spin-polarized, and the distance between reconstructed OIII pairs is 1.5 Å, which matches with O_2^{2-} molecule [39]. The phase of non-stoichiometric surface oxygen pairs can be attributed to the XPS peak at 532.1 eV. This assumption correlates with results discussed in [39] where XPS peak at 532 eV is attributed to the molecular oxygen ions on oxidized metal surface. The high temperature annealing of the indium oxide films restored the surface stoichiometry, which was reflected in proportional increase of the peak at 530.5 eV corresponding to lattice oxygen and decrease of the peak at 532.1 eV during the surface treatment (Fig. 6b). In computational investigations, oxygen pairs were noticed to be stabilized also at lower oxygen coverages (below 0.04 $Å^{-2}$), but stability is significantly lower (adsorption energy 0.6 eV/atom).

Unsaturated In ions, which appear at oxygen-deficient surface, are expected to serve as the surface sites for chemisorbed oxygen and water related species. The adatoms stabilized at the unsaturated indium ions provide a path for "redox" realization of chemisorption and catalysis at the real surface of In_2O_3. On the other hand, the different oxygen forms found on the surface can be involved in reactions producing reactive oxygen species (O^- and O_2^-) at the surface. Considering ozone detection, related theoretical calculations do not support stabilization of oxygen pairs on perfect tin dioxide surface [40]. Thus, there can be a fundamental reason for the superiority of In_2O_3 to ozone detection, as decomposition of ozone molecule is expected to be mediated through a formation of oxygen pair [41].

Table 1
Limits of the surface energies (E_{surf}) for the (4 0 0) In_2O_3 atomic face with different coverage of surface bridging oxygens

Surface	Oxidation coverage ($Å^{-2}$)	E_{surf} O_2-rich (J/m^{-2})	E_{surf} In-rich (J/m^{-2})
OII + OIII	0.08	1.6	2.4
OI + OIII	0.08	2.1	2.9
OI + OII	0.08	2.2	3.0
OIII	0.04	2.3	1.5
OII	0.04	2.3	1.5
OI	0.04	2.4	1.6
Reduced	0.00	3.2	0.8

5. Conclusions

The conducted study of In_2O_3 films deposited by spray pyrolysis permits us to conclude that response time of In_2O_3-based gas sensors to oxidizing gases is limited by diffusion type processes. Mechanisms of In_2O_3 sensitivity to reducing gases include "redox" and catalytic effects in a thin subsurface layer. The perfect In_2O_3 (4 0 0) surface with full oxygen coverage is found to stabilize by forming oxygen

molecules that are only weakly bound to surface. The surface reconstruction connected with the symmetry breakdown of bridging oxygen atoms of the terminal layer leads to formation of energetically stable non-stoichiometric surface featured by deficiency of lattice oxygen. Mono-oxygen and also di-oxygen species form and stabilize at the surface with sufficient oxygen coverage. Based on computational investigations, the bond length of the di-oxygen corresponds to that of $O_2{}^{2-}$. The surface energies between 1.5 and 2 J/m^2 are evaluated for the reconstructed OIII and OII + OIII surface models, with adsorption energies between 1.2 and 1.4 eV/oxygen. The oxygen adatoms stabilized at the unsaturated indium ions are predicted to provide a path for competitive realization of the chemisorption and catalytic mechanisms at real surface of In_2O_3.

Acknowledgements

This work was supported by EC in the frame of INTAS Program (Grants INTAS – 2001-0009 and 2000-0066). We are thankful to V. Matolin and A. Cirera for help in conducting XPS and Raman spectroscopy experiments, correspondingly. The authors would like to thank the Graduate school of functional surfaces (The Academy of Finland) for support and the Center for Scientific Computing (CSC, Finland), for computational resources.

References

[1] C. Cantalini, W. Wlodarski, H.T. Sun, M.Z. Atashbar, M. Passacantando, A.R. Pheni, S. Santucci, Investigation on the cross sensitivity of NO_2 sensors based on In_2O_3 thin films prepared by sol–gel and vacuum thermal evaporation, Thin Solid Films 350 (1999) 276–282.

[2] H. Steffes, C. Imawan, F. Solzbacher, E. Obermeir, Enhancement of NO_2 sensing properties of In_2O_3-based thin films using an Au or Ti surface modification, Sens. Actuators B 78 (2001) 106–112.

[3] H. Yamaura, K. Moriya, N. Miura, N. Yamazoe, Mechanism of sensitivity promotion in CO sensor using indium oxide and cobalt oxide, Sens. Actuators B 65 (2000) 39–41.

[4] Y. Boris, G. Korotcenkov, V. Brinzari, M. Ivanov, Yu. Lychkovsky, G. Karkotsky, V. Golovanov, A. Cornet, E. Rossyniol, Influence of In_2O_3 doping on gas response to CO and H_2, Proceedings of the Third International Conference on Microelectronics and Computer Science ICMCS-02, 26–28 September, Chisinau, Moldova, 2002, pp. 344–347.

[5] A. Gurlo, N. Barsan, M. Ivanovskaya, U. Weimar, W. Gopel, In_2O_3 and MoO_3-In_2O_3 thin film semiconductor sensors: interaction with NO_2 and O_3, Sens. Actuators B 47 (1998) 92–99.

[6] E. Gagaoudakis, M. Bender, E. Duloufakis, N. Katsarakis, E. Natsakou, V. Cimalla, G. Kiriakidis, The influence of deposition parameters on room termperature ozone sensing properties of InO_x films, Sens. Actuators B 80 (2001) 155–161.

[7] S.R. Kim, H.K. Hong, C.H. Kwon, D.H. Yun, K. Lee, Y.K. Sung, Ozone sensing properties of In_2O_3-based semiconductor thick films, Sens. Actuators B 66 (2000) 59–62.

[8] T. Takada, Ozone Detection by In_2O_3 Thin Film Gas Sensor in: T. Seiyama (Ed.), Chemical Sensor Technology, vol. 2, Kodansha, Tokyo, 1989, pp. 59–70.

[9] A. Gurlo, M. Ivanovskaya, A. Fuchs, T. Doll, I. Eisele, W. Gopel, Conductivity and work function of nanocrystalline In_2O_3 and In_2O_3-MoO3 sensors for ozone detection, in: Proceedings of the Eurosensors XII, Southampton, UK, 13–16 September, 1998, pp. 621–624.

[10] S.N. Malchenko, Y.N. Lychkovski, M.V. Baykov, One-electrode semiconductor sensor for detection of toxic and explosive gases in air, Sens. Actuators B 7 (1992) 505–506.

[11] V. Golovanov, J.L. Solis, V. Lantto, S. Leppavuori, Different thick-film methods in printing of one-electrode semiconductor gas sensors, Sens. Actuators B 34 (1996) 1–6.

[12] V. Lantto, V. Golovanov, Y. Lychkovsky, Carbon monoxide monitoring in combustion emissions using SnO_2 and In_2O_3 gas sensors, in: The Proceedings of the TTFS'94 Workshop, Szklarsla Poreba, Poland, 13–16 September, 1994, pp. 180–183.

[13] A. Gurlo, M. Ivanovskaya, N. Barsan, M. Schwerzer-Berberich, U. Weimar, W. Gopel, A. Dieguez, Grain size control in nanocrystalline In_2O_3 semiconductor gas sensors, Sens. Actuators B 44 (1977) 327–333.

[14] W.-Y. Chung, G. Sakai, K. Shimanoe, N. Miura, D.-D. Lee, N. Yamazoe, Preparation of indium oxide thin film by spin-coating method and its gas sensing properties, Sens. Actuators B 46 (1998) 139–145.

[15] A. Galdikas, Z. Martunas, A. Setkus, SnInO-based chlorine gas sensor, Sens. Actuators B 7 (1992) 633–636.

[16] A.P. Mammana, E.S. Braga, I. Torriani, R.P. Anderson, Structural characterisation of transparent semiconducting thin films of SNO_2 and In_2O_3, Thin Solid Films 85 (1981) 355–359.

[17] D. Manno, M. Di Giulio, T. Siciliano, E. Filippo, A. Serra, Structural and electrical properties of In_2O_3/SeO_2 thin films for gas-sensing applications, J. Phys. D Appl. Phys. 34 (2001) 2097–2102.

[18] M. Asikainen, M. Ritala, T. Leskela, G. Prohaska, M. Friedbacher, Grasserbauer, AFM and STM studies on In_2O_3 and ITO thin films deposited by atomic layer epitaxy, Appl. Surf. Sci. 99 (1996) 91–98.

[19] F.O. Adurodija, H. Izumi, T. Ishihara, H. Yoshioka, M. Motoyaman, K. Murai, Influence of substrate temperature on the properties of indium oxide thin films, J. Vac. Sci. Technol. A 18 (2000) 814–817.

[20] H. Yamaura, T. Jinkawa, J. Tamaki, K. Moriya, N. Miura, N. Yamazoe, Indium oxide-based gas sensors for selective detection of CO, Sens. Actuators B 35–36 (1996) 325–332.

[21] S. Poznyak, A. Golubev, A. Kulak, Correlation between surface properties and photocatalytic and photoelectrochemical activity of In_2O_3 nanocrystalline films and powders, Surf. Sci. 454–456 (2000) 396–401.

[22] M. Ivanovskaya, P. Bogdanov, G. Faglia, G. Sberveglieri, Properties of thin film and ceramic sensors for the detection of CO and NO_2, in: Proceedings of the International Conference on Eurosensors XIII, Hague, The Netherlands, 12–15 September, 1999, pp. 145–148.

[23] M. Ivanovskaya, P. Bogdanov, N. Barsan, J. Kappler, The influence of humidity on a sensitive behavior of In_2O_3-based sensors, in: The Proceedings of the Eurosensors XIV, Copenhagen, Denmark, 27–30 August, 2000, pp. 149–151.

[24] P. Bogdanov, M. Ivanovskaya, The effect of In_2O_3-SNO_2 structure on the properties of ceramic sensors, in: Proceedings of the Eurosensors XI, Warsaw, Poland, 21–24 September, 1997, pp. 309–312.

[25] G. Korotcenkov, A. Cerneavschi, V. Brinzari, A. Cornet, J. Morante, A. Cabot, J. Arbiol, Crystallographic characterization of In_2O_3 films deposited by spray pyrolysis, Sens. Actuators B 84 (2002) 37–42.

[26] G. Korotcenkov, V. Brinzari, A. Cerneavschi, M. Ivanov, V. Golovanov, A. Cornet, The influence of film structure on In_2O_3 gas response, Thin Solid Films 460 (2004) 315–323.

[27] V. Brinzari, G. Korotcenkov, V. Golovanov, Factors influencing the gas sensing characteristics of tin dioxide films deposited by spray pyrolysis: understanding and possibilities for control, Thin Solid Films 391 (2001) 167–175.

[28] Y. Boris, G. Korotcenkov, V. Brinzari, Yu. Lychkovsky, G. Karkotsky, V. Golovanov, Gas sensing characteristics of doped In_2O_3 gas sensors, in: The Proceedings of the Third International Conference

on “Microelectronics and Computer Science” ICMCS-02, Chisinau, Moldova, 26–28 September, 2002, pp. 340–343.
[29] T.M. Ratcheva, M.D. Nanova, L.V. Vassilev, M.G. Mikhailov, Properties of In_2O_3:Te films prepared by the spraying method, Thin Solid Films 139 (1986) 189–199.
[30] R.I.R. Blyth, F.P. Netzer, M.G. Ramsey, Photoemission study of In_2O_3 thin films on NiIn (0 0 0 1): valence bonds and midium 4d levels of a model far ITO, Surf. Sci. 465 (2000) 120–126.
[31] Joint Commitee on Powders Diffraction Standards. Card 6-416. JCPDS International Center for Diffraction Data. Swarthmore, USA.
[32] G. Korotcenkov, A. Cerneavschi, V. Brinzari, A. Palagnuk, A. Cornet, J. Morante, A. Cabot, J. Arbiol, In_2O_3 films deposited by spray pyrolysis as a material for ozone gas sensors, Moldavian J. Phys. Sci. 1 (2002) 24–29.
[33] G. Korotcenkov, V. Brinzari, A. Cerneaschi, M. Ivanov, Kinetics of In_2O_3 gas response, in: Third International Seminar on Semiconductor Gas Sensors, Ustron, Poland, 2002, p. 47. Abstracts.
[34] V. Milman, B. Winkler, J.A. White, C.J. Pickard, M.C. Payne, E.V. Akhmatskaya, R.H. Nobes, Electronic structure, properties, and phase stability of inorganic crystals: a pseudopotential plane-wave study, Int. J. Quant. Chem. 77 (2000) 895–899.
[35] D. Vanderbilt, Soft self-consistent pseudopotentials in a generalized eigenvalue formalism, Phys. Rev. B 41 (1990) 7892–7895.
[36] H.J. Monkhorst, J.D. Pack, Special points for brillouin-zone-integrations, Phys. Rev. B 13 (1976) 5188–5192.
[37] J.P. Pedrew, Y. Wang, Atoms, molecules, solids and surfaces: applications of the generalized gradient approximation for exchange and correlation, Phys. Rev. B 46 (1992) 6671–6687.
[38] M.A. Mäki-Jaskari, T.T. Rantala, Theoretical study of oxygen deficient SNO_2(1 1 0) surfaces, Phys. Rev. B 65 (2002) 245–428.
[39] M. Che, A.J. Tench, Characterization and reactivity of molecular oxygen species on oxide surfaces, Adv. Catal. 32 (1983) 1.
[40] V.V. Golovanov, M.A. Mäki-Jaskari, T.T. Rantala, Semi-empirical and ab-initio studies of low-temperature adsorption of oxygen and CO at (1 1 0) face of SnO_2, IEEE Sens. J. 2 (2002) 416–421.
[41] B. Dhandapani, S.T. Oyama, Gas phase ozone decomposition catalysts, Appl. Catal. B 11 (1997) 129–166.

Biographies

Vyacheslav Golovanov received M.Sc. degree in material science from Odessa State University in 1983, Ph.D. degree from Odessa State University in 1988 and Dr.Sc degree from the same University in 1998 for studies in the fields of surface physics, solid-gas interfaces and physics of semiconductors. Presently he is a Professor at the Faculty of Physics, South-Ukrainian University and Head of Sensors Electronics & Technology Laboratory aimed activities in manufacturing of semiconductor gas instruments. His current research interests focuses on ab initio study of chemisorption and catalytic effects on the surface of semiconductors, sensor systems for environmental monitoring.

Matti Mäki-Jaskari received M.Sc. degree in applied physics from the Department of Engineering, Physics and Mathematics, Helsinki University of Technology, Helsinki, Finland. He is currently pursuing the Ph.D. degree at the Semiconductor Physics Laboratory, Tampere University of Technology, Tampere, Finland. His work is focused on atomistic modeling of materials.

Tapio Tuomas Rantala received the M.Sc. degree in physics in 1978, the M.Sc. degree in technical physics (materials science) in 1984, and the Ph.D. degree in physics for DFT studies on metals and metal surfaces in 1987, all from the University of Oulu, Finland. Currently, he is a Professor of physics and the Head of the Semiconductor Physics Laboratory, Institute of Physics, Tampere University of Technology, Tampere, Finland. His current research interests include theoretical and computational studies of compound semiconductors and their surfaces and interfaces, in particular.